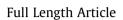
Fuel 203 (2017) 32-46

Contents lists available at ScienceDirect

Fuel

journal homepage: www.elsevier.com/locate/fuel



Pore connectivity and tracer migration of typical shales in south China

Mengdi Sun^{a,b}, Bingsong Yu^{a,*}, Qinhong Hu^{b,*}, Rui Yang^{c,*}, Yifan Zhang^a, Bo Li^a

^a School of Earth Sciences and Resources, China University of Geosciences (Beijing), Beijing 100083, China

^b Department of Earth and Environment Sciences, University of Texas at Arlington, Arlington, TX 76019, USA

^c Key Laboratory of Tectonics and Petroleum Resources, Ministry of Education, China University of Geosciences, Wuhan 430074, China

HIGHLIGHTS

• Experimental studies were conducted on pore connectivity and wettability of shale.

• Pore connectivity was studied using imbibition, diffusion, MICP, and FE-SEM.

• Multiple factors influencing pore connectivity were discussed.

• Pore connectivity of gas shales will affect hydrocarbon preservation and recovery.

ARTICLE INFO

Article history: Received 28 February 2017 Received in revised form 15 April 2017 Accepted 19 April 2017

Keywords: Shale gas Pore structure Connectivity Wettability Imbibition

ABSTRACT

Pore connectivity of shale is a critical factor in shale gas migration and production. In order to investigate the pore connectivity from three typical shale formations in south China (Longmaxi, Niutitang, and Longtan shales), we conducted complementary analyses with field emission-scanning electron microscopy (FE-SEM), mercury intrusion capillary pressure (MICP), gas (CO₂ and N₂) sorption isotherm, contact angle, spontaneous imbibition, as well as saturated diffusion with tracer distribution mapped with laser ablation-inductively coupled plasma-mass spectrometry. The use of water and n-decane fluids enables us to examine the connectivity of hydrophilic and hydrophobic pore networks of the shale, and the resultant imbibition slopes demonstrate that Longmaxi shale has a high connectivity from its high-development of both well-connected organic and inorganic pores. Limited diffusion distances and associated high tortuosity (from both diffusion and MICP analyses) are consistent with the predominant presence of nanosized pore throats (3–50 nm) from gas sorption isotherm and MICP tests. Pore types, development degree, and connection are directly supported by FE-SEM-imaging. Overall, the variable and limited pore connectivity of shale samples will affect hydrocarbon preservation and recovery.

© 2017 Elsevier Ltd. All rights reserved.

1. Introduction

The ongoing 'shale revolution' in United States has triggered worldwide interest about shale gas exploration and exploitation [1]. As a relatively clean fossil fuel, shale gas will reduce the fuel need for foreign imports to accommodate the booming economy in China. In addition to sandstone and carbonate, shale formations have gradually been recognized to be important hydrocarbon reservoirs [2]. Nearly all producing shale gas plays in US are marine

formation. However, there are three types of organic-rich shale formations in China (by area: marine shale 26%, marine-terrestrial transitional shale 56%, and lacustrine shale 18%) [3,4]. Sinopec reported that the Fuling marine shale gas field in Sichuan Basin of China produced $31.67 \times 10^8 \text{ m}^3$ in 2015, after achieving in 2014 the first shale gas commercial production after North America [5,6].

Horizontal drilling and hydraulic fracturing are key technologies in shale gas development [1]. Hydraulic fracturing allows gas molecules to move into the new fractures from the shale matrix, wherein the mass transfer process is mainly by matrix diffusion. Meanwhile, pore connectivity in shale can affect matrix diffusion, and limit the gas production rate and hydrocarbon recovery [7–9]. Studies about the geometrical attributes of pore structure such as pore shape, size, and distribution in shale have been heavily reported in the literature [10–13]. However, the research of







^{*} Corresponding authors at: School of Earth Sciences and Resources, China University of Geosciences (Beijing), Beijing 100083, China (B. Yu); Department of Earth and Environment Sciences, University of Texas at Arlington, Arlington, TX 76019, USA (Q. Hu); Key Laboratory of Tectonics and Petroleum Resources, Ministry of Education, China University of Geosciences, Wuhan 430074, China (R. Yang).

E-mail addresses: yubs@cugb.edu.cn (B. Yu), maxhu@uta.edu (Q. Hu), yangyingrui@163.com (R. Yang).

pore connectivity in shale matrix, the topological aspect of pore structure, is poorly documented and understood.

The connectivity of nano-sized pores in shale matrix controls the accessible porosity and matrix diffusion rate [14–16]. Hu et al. reported that low pore connectivity of Barnett Shale caused low overall recovery and dramatic decline in gas production [7]. The neutron scattering results of Barnett Shale indicate that the accessible porosities to methane and water are different, even though the total porosity does not differ [14]. It is found that a disconnected pore network commonly occurs in formations with low porosity and low permeability [17,18]. The pore network in organic shale is generally a complex mingling of hydrophobic organic pores and hydrophilic inorganic pores. Previous studies demonstrated that the wettability of pore spaces affects the connectivity of hydrophobic and hydrophilic pore networks [19–21].

In order to elucidate the pore connectivity in shale matrix, various methods have been utilized in recent literature. Three dimensional (3D) pore networks were reconstructed by nano-computed tomography (nano-CT), nano-transmission X-ray microscopy (nano-TXM), and focused ion beam-scanning electron microscopy (FIB-SEM) techniques to analyze the geometry and connectivity of pore networks [11,22]. The pore connectivity can also be assessed by evaluating the difference of porosities determined from small angle neutron scattering (SANS), mercury injection capillary pressure (MICP) and helium pycnometry [23–25]. Spontaneous imbibition test is another simple and useful method to characterizing the pore connectivity and wettability of shale samples [26–31], be assessing the imbibition slope of the log cumulative imbibition versus log imbibition time [7,8,18].

The purpose of this work was to investigate the controlling factors (pore types and development degree, pore size distribution, tortuosity, and wettability) on pore connectivity. Both deionized water (hydrophilic) and n-decane (hydrophobic) were used as imbibing fluids in spontaneous imbibition tests, to complement with a combination of FE-SEM, MICP, and low-pressure N_2/CO_2 sorption isotherm analyses. In addition, LA-ICP-MS (laser ablation-inductively coupled plasma-mass spectrometry) was applied to investigate the diffusion behavior of a nonsorbing tracer by mapping the tracer distribution in shale samples initially saturated with brine.

2. Shale samples and methods

2.1. Sample collection and analyses

Six core shale samples from the Lower Cambrian marine Niutitang formation, the Lower Silurian marine Longmaxi formation and the Upper Permian marine-terrestrial transitional Longtan formation in south-west China were collected for analyses of pore connectivity and tracer migration behavior. Their depth, geologic ages, total organic carbon (TOC) and maturation levels (R_o) are listed in Table 1. All the wells are distributed on the southeast and southern margins around Sichuan Basin (Fig. 1). Based on previous studies of shale gas reservoirs in south China [32–36], six

I dDIC I						
Properties	of shale	samples	used	in	this	work.

Table 1

shale core samples were chosen from these three important formations of shale gas exploration, taking into consideration the variability of TOC, maturity, and mineral composition. Therefore, the tested samples can reasonably represent the typical shale formations in south China. Meanwhile, core samples used for analyses were massive and well preserved. The subsamples taken from core samples are as homogeneous as possible so that analyses made on subsamples can be correlated.

2.2. Mineralogy

Shale samples were first crushed into powder less than 200 mesh in size, and then separated for clay minerals by using a gravity method. X-ray diffraction (XRD) analyses were performed on powdered shale and clay minerals using a Bruker instrument with a step of 0.02° from 2° to 70° at room temperature of 20 °C. The bulk mineral composition and relative content of clay minerals were semi-quantified with Jade[®] 6.0 software. Illite crystallinity was calculated from the half high-width of maximum diffraction intensity of illite's diffraction peak at 10 Å.

2.3. Field emission-scanning electron microscopy and polarized light microscopy imaging

llion⁺ II (Model 697, Gatan) was used to produce a smooth surface, and subsequently 10 nm thick gold was coated on the surface to enhance the electrical conductivity to observe the microstructure morphology with FE-SEM (Zeiss SUPPA 55).

To characterize the texture, fabric, and mineralogy, we prepared thin (<0.03 mm) polished sections for each sample. These thin sections were then analyzed by polarized light microscopy to capture their microtextural and compositional attributes.

2.4. Low-pressure gas sorption isotherm and mercury injection capillary pressure analyses

Quantitative pore structure characteristics of these samples were investigated by MICP, as well as both nitrogen and carbon dioxide sorption isotherm experiments with the approaches published in our previously work [13]. MICP analyses were carried out with AutoPore IV 9510 (Micromeritics) at pressures from 0.034 MPa to 413 MPa (5 to 60000 psi; 1 MPa = 145 Psi), corresponding to a low-limit detection of pore throat diameter of approximately 3 nm based on Washburn equation [37]. Prior to the MICP test, each shale sample (1 cm-sized cube) was ovendried at 60 °C for at least 48 h to remove moisture in pore spaces, and then cooled to approximately 23 °C (room temperature) in a desiccator with a relative humidity less than 10%. The porethroat diameter distribution for each intrusion/extrusion pressure is directly obtained through the physical constants for mercury on geological materials: surface tension, $\gamma = 485$ mN/m, and contact angle, $\theta = 130^{\circ}$ [38].

Sample	Well	Depth (m)	Geologic Age	Formation	Deposition	TOC (wt.%)	R _o * (%)
XY1-90	XY1	637.2	Early Silurian	Longmaxi	Marine	3.72	2.17
XY1-96	XY1	643.2	Early Silurian	Longmaxi	Marine	4.88	2.21
TY1-14	TY1	670	Early Silurian	Longmaxi	Marine	7.58	2.12
YK1-48	YK1	44.9	Early Cambrian	Niutitang	Marine	7.96	3.22
RY2-16	RY2	922.5	Early Cambrian	Niutitang	Marine	9.99	3.39
(X)Y1-1	(X)Y1	549	Late Permian	Longtan	Transitional	8.53	2.82

TOC = total organic carbon; R_o° = equivalent vitrinite reflectance converted from the reflectance of bitumen.

Download English Version:

https://daneshyari.com/en/article/6474262

Download Persian Version:

https://daneshyari.com/article/6474262

Daneshyari.com